Supplemental Material for

Multiferroicity in 2D MSX$_2$ (M = Nb and Zr; X = Cl, Br, and I)

Yutong Li[1,2], Haoyun Bai[2], Zhichao Yu[2], Chi Tat Kwok[1,2*], and Hui Pan[2,3*]

[1] Department of Electromechanical Engineering, Faculty of Science and Technology, University of Macau, Macao SAR, China

[2] Institute of Applied Physics and Materials Engineering, University of Macau, Macao SAR, China

[3] Department of Physics and Chemistry, Faculty of Science and Technology, University of Macau, Macao SAR, China

*Corresponding authors:

C. T. Kwok: fstctk@um.edu.mo (email)
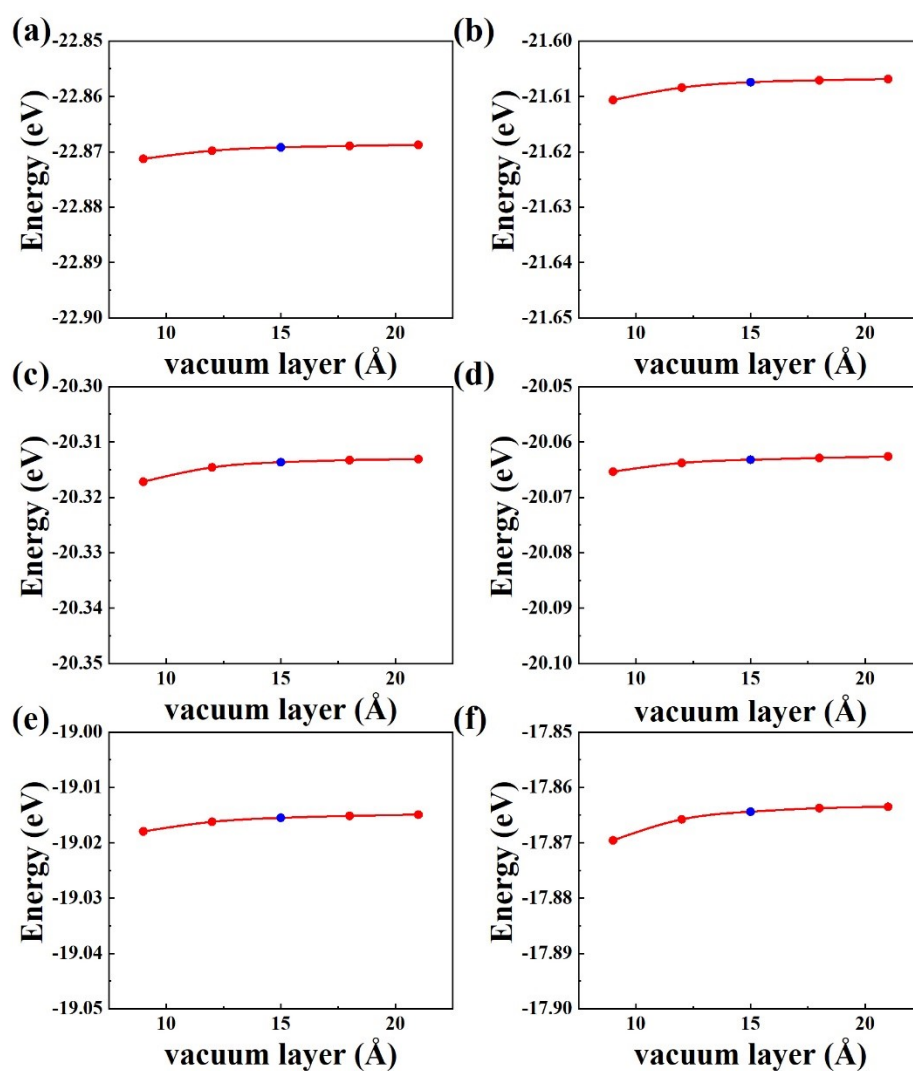
H. Pan: huipan@um.edu.mo (email)

Figure S1 The total energy as a function of thickness of vacuum layer in (a) ZrSCl$_2$, (b) ZrSBr$_2$, (c) ZrSI$_2$, (d) NbSCl$_2$, (e) NbSBr$_2$, (f) NbSI$_2$. The vacuum layers used in our calculations is marked in blue blocks.
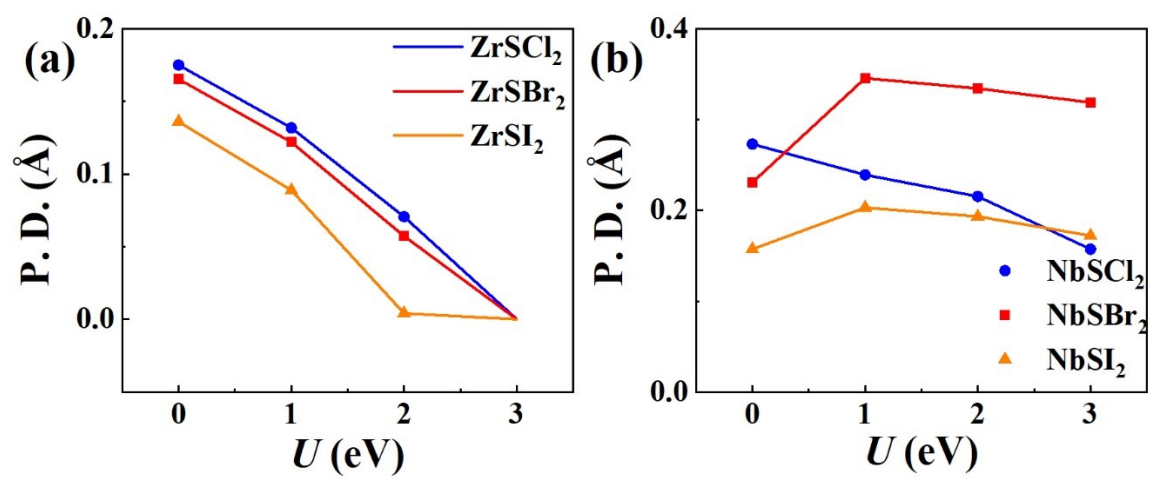
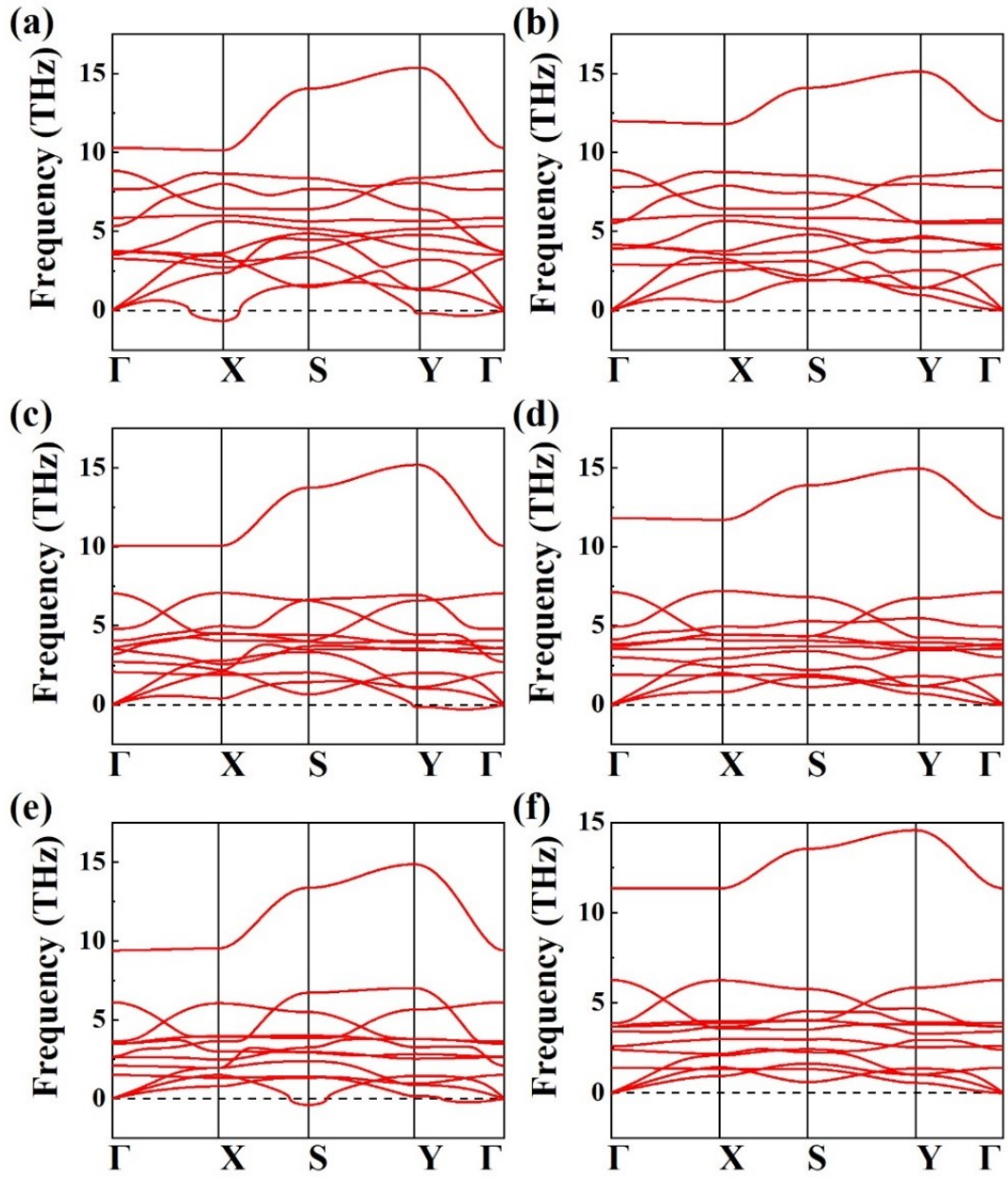Figure S2 P. D. of (a) $ZrSX_2$ (b) $NbSX_2$ with different U values.

Figure S3 Phonon dispersions: FE ZrSCl$_2$ (a) without and (b) with a tension of 5% along the *b*-axis; FE ZrSBr$_2$ (c) without and (d) with a tension of 5% along the *b*-axis; FE ZrSI$_2$ (e) without and (f) with a tension of 5% along the *b*-axis.
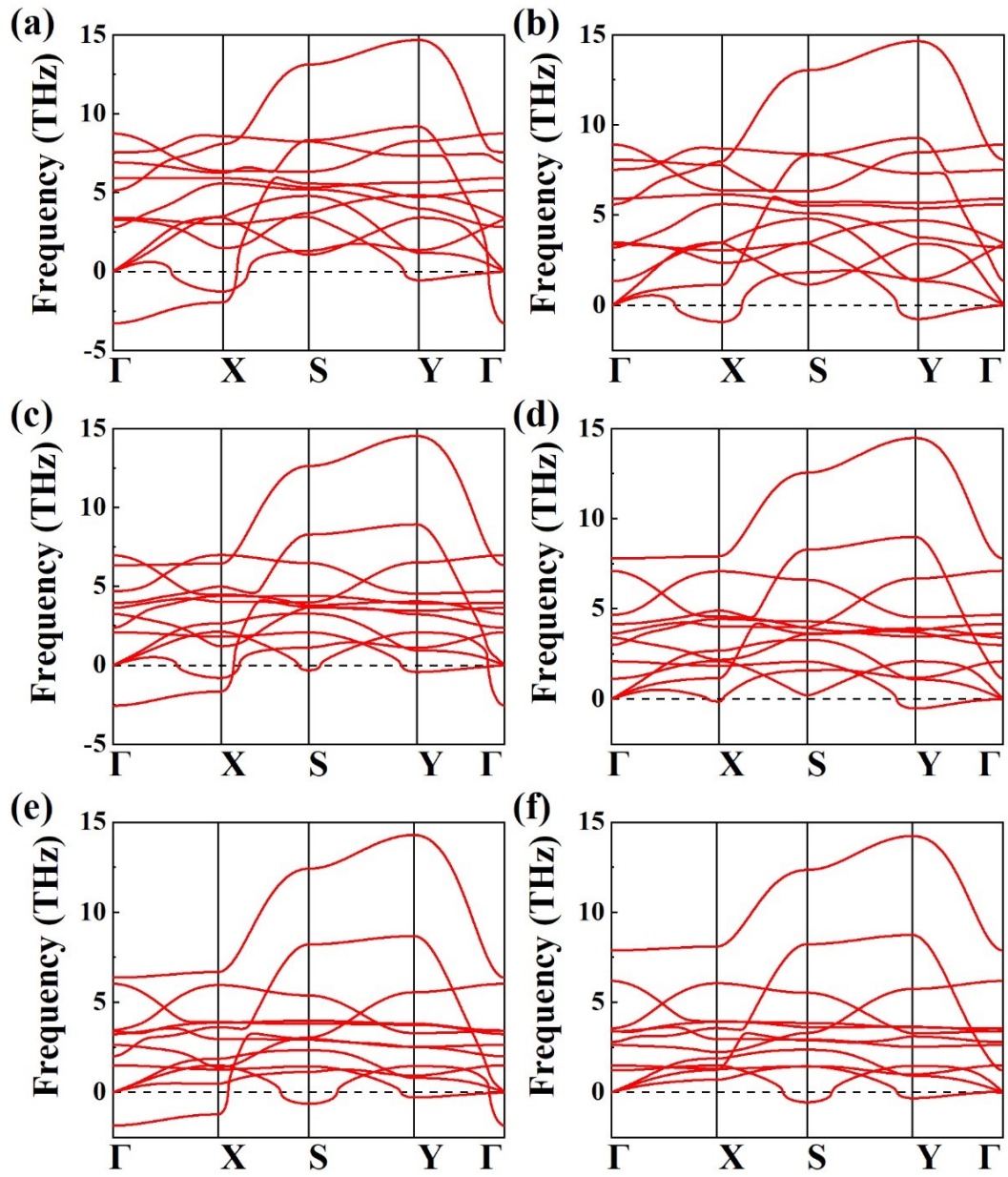
Figure S4 Phonon dispersions: PE ZrSCl$_2$ (a) without and (b) with $U = 3$ eV; PE ZrSBr$_2$ (c) without and (d) with $U = 3$ eV; PE ZrSI$_2$ (e) without and (f) with $U = 3$ eV.
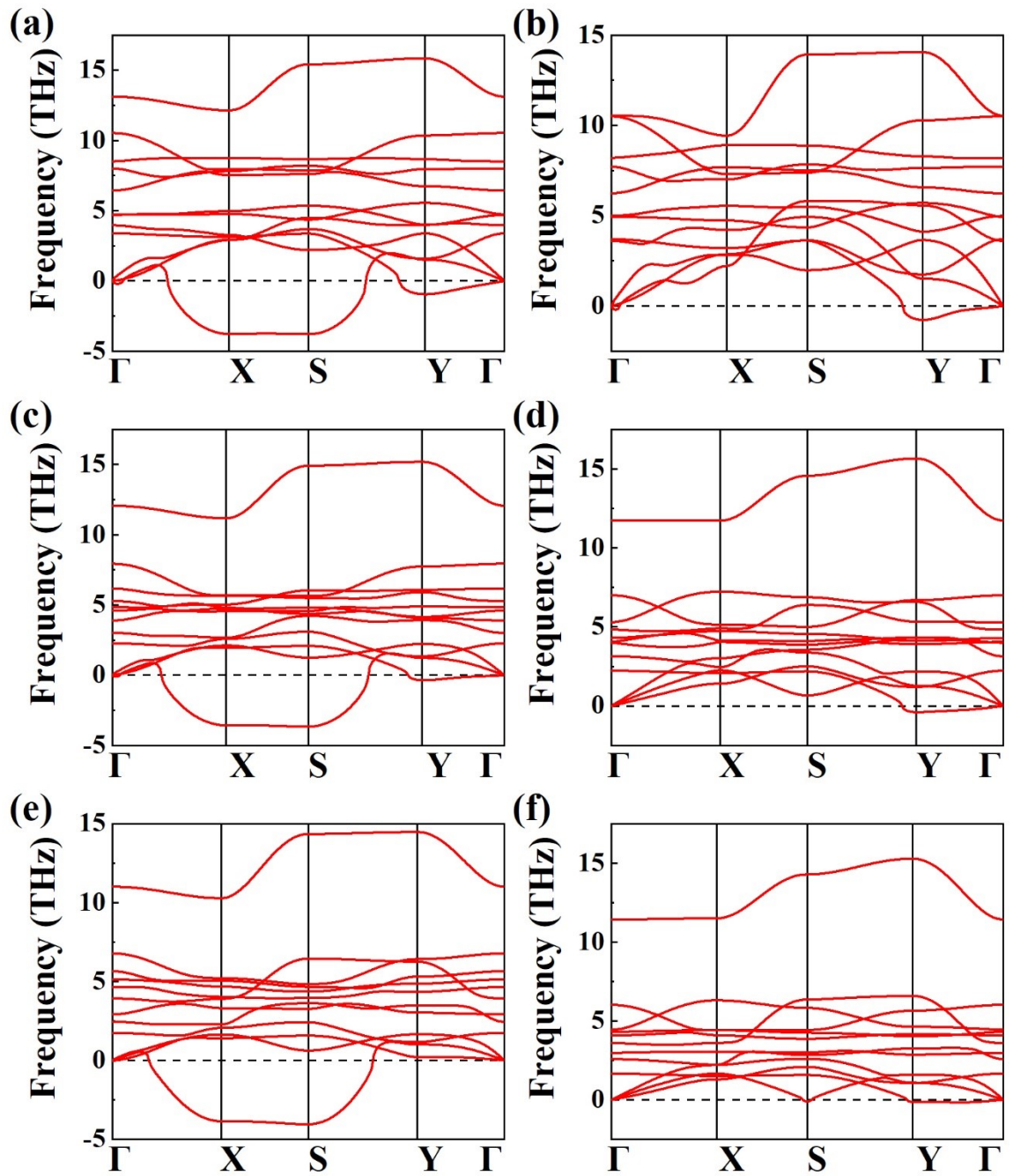
Figure S5 Phonon dispersions: FE NbSCl$_2$ (a) without and (b) with $U = 3$ eV; FE NbSBr$_2$ (c) without and (d) with $U = 3$ eV; FE NbSI$_2$ (e) without and (f) with $U = 3$ eV.
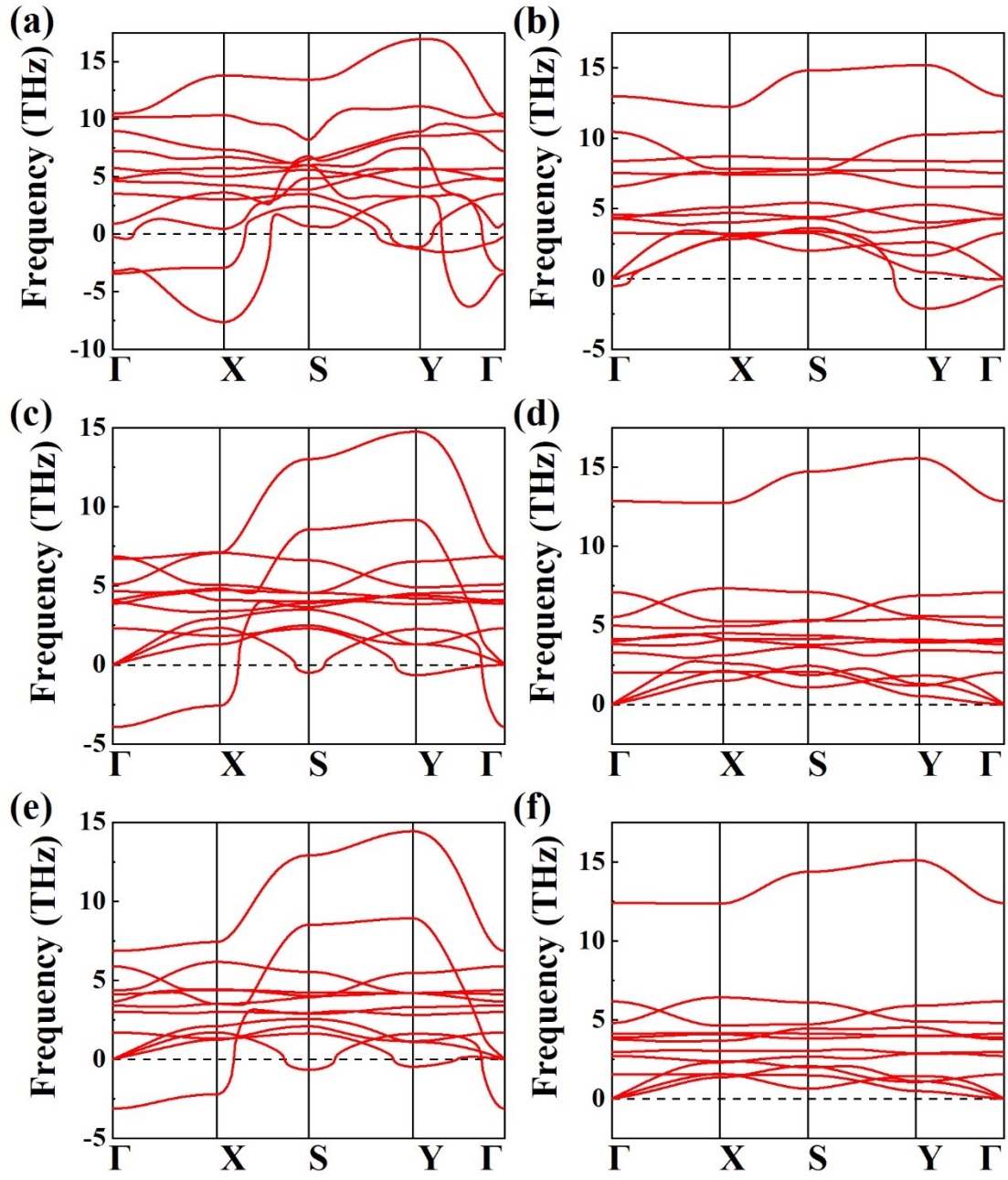
Figure S6 Phonon dispersions at $U = 3$ eV under a tension of 5% along the b-axis: (a) PE and (b) FE NbSCl$_2$; (c) PE and (d) FE NbSBr$_2$; (e) PE and (f) FE NbSI$_2$.
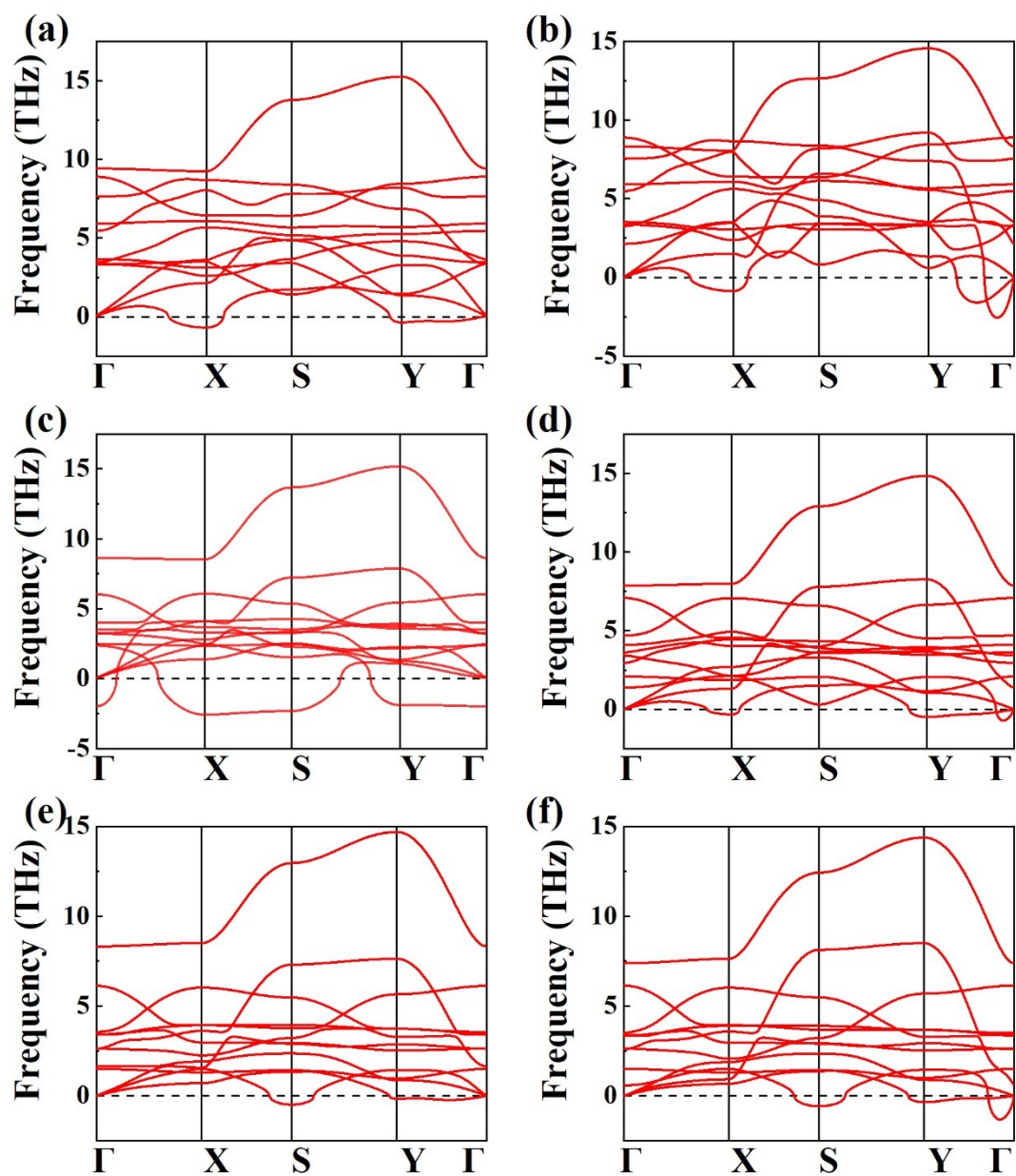
Figure S7 Phonon dispersions: FE ZrSCl$_2$ (a) with $U = 1$ eV and (b) $U = 2$ eV; FE ZrSBr$_2$ (c) with $U = 1$ eV and (d) $U = 2$ eV; FE ZrSI$_2$ (e) with $U = 1$ eV and (f) $U = 2$ eV.

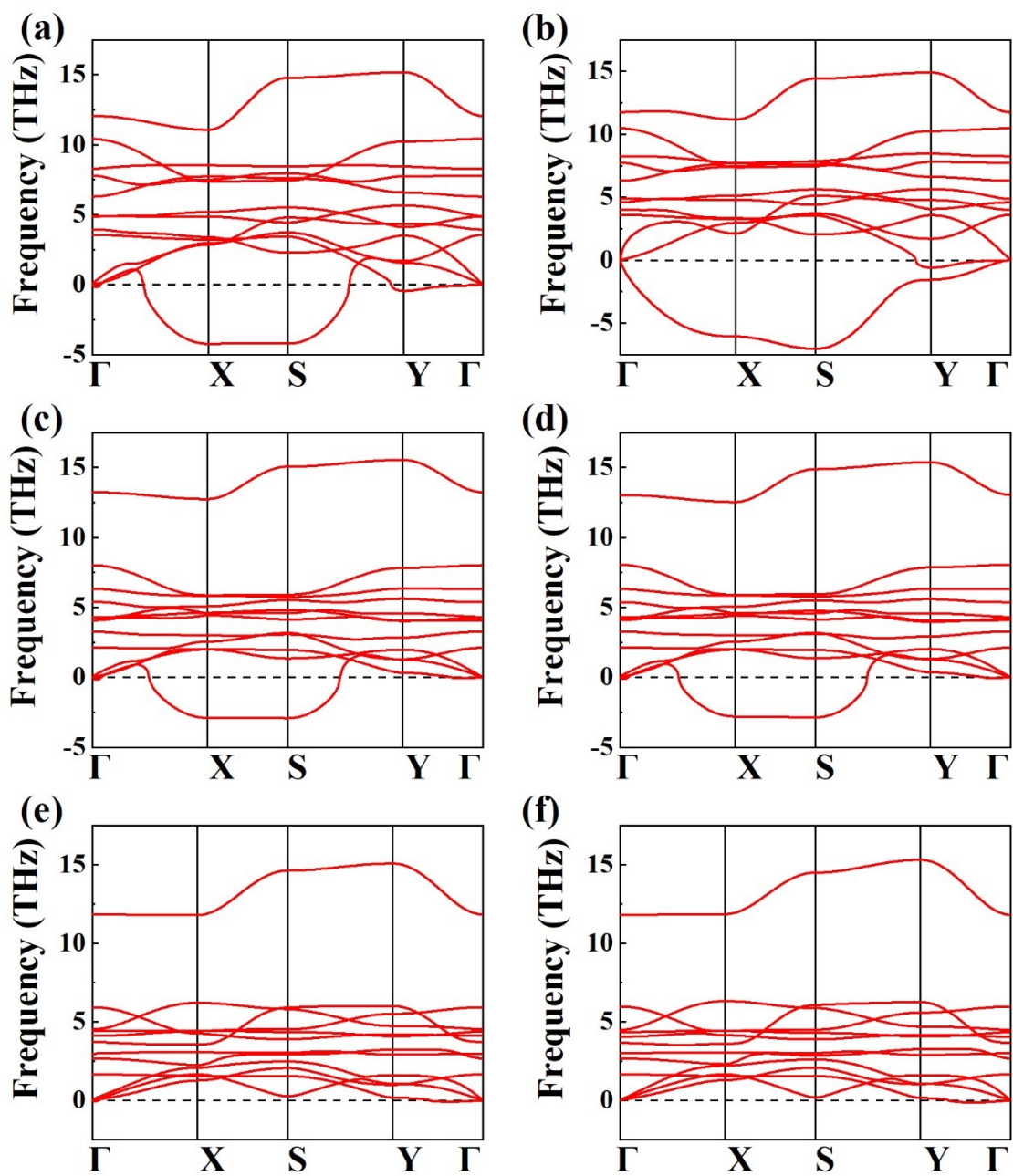Figure S8 Phonon dispersions: FE NbSCl$_2$ (a) with $U = 1$ eV and (b) $U = 2$ eV; FE NbSBr$_2$ (c) with $U = 1$ eV and (d) $U = 2$ eV; FE NbSI$_2$ (e) with $U = 1$ eV and (f) $U = 2$ eV.
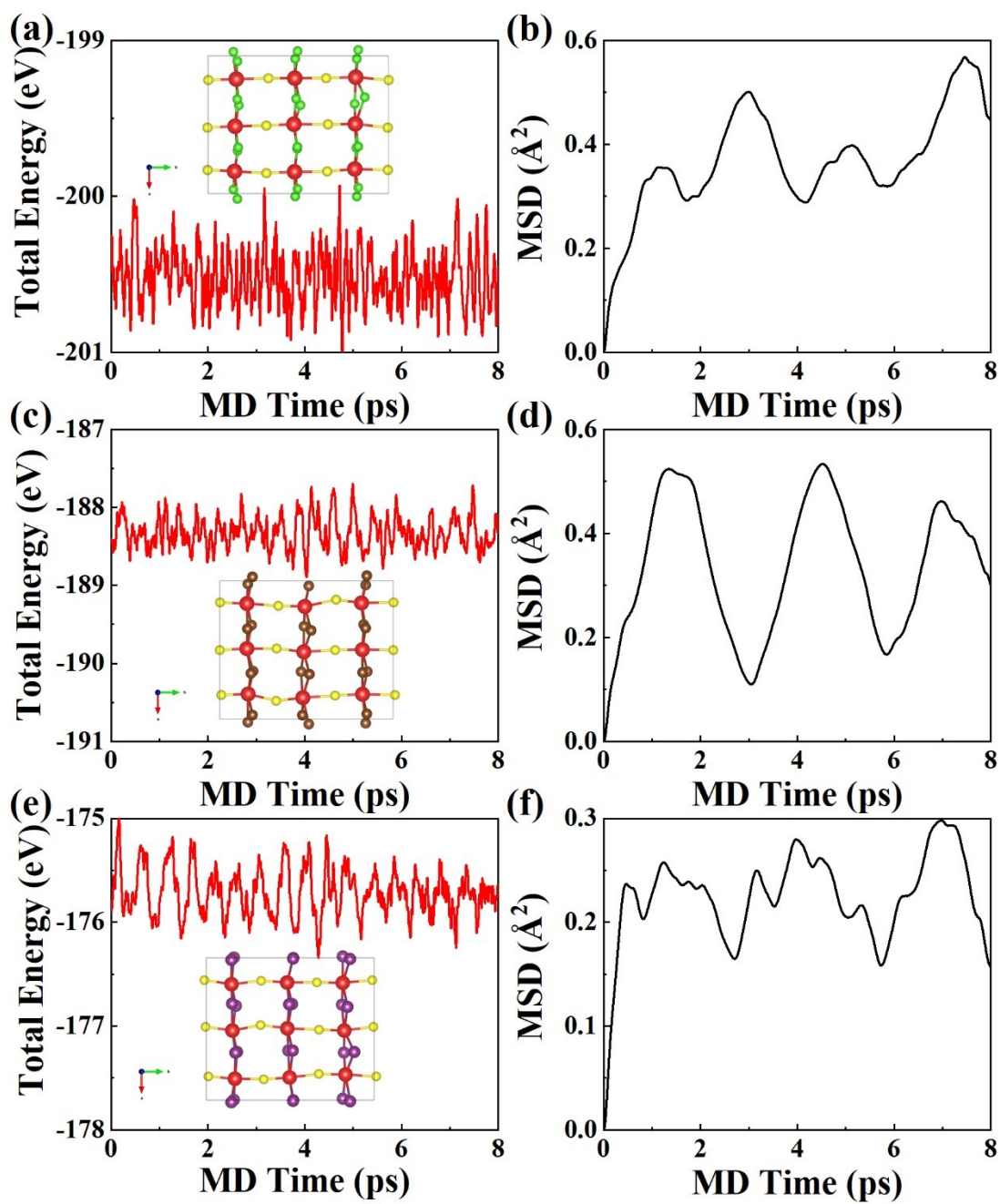
Figure S9 (a) The total energies and (b) the MSDs of ZrSCl$_2$, (c) the total energies and (d) the MSDs of ZrSBr$_2$, and (e) the total energies and (f) the MSDs of ZrSI$_2$ during the AIMD simulations.
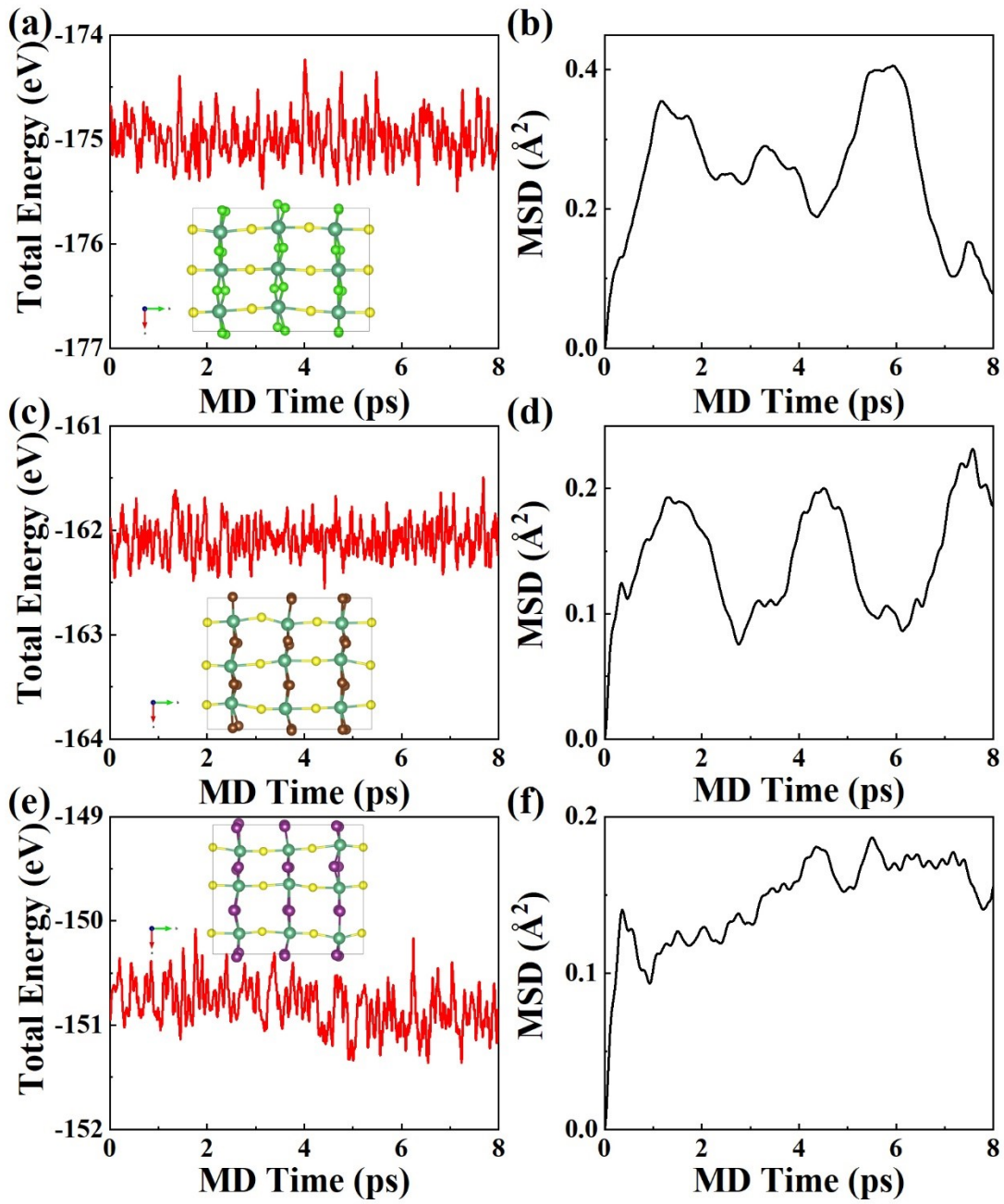
Figure S10 (a) The total energies and (b) the MSDs of NbSCl$_2$, (c) the total energies and (d) the MSDs of NbSBr$_2$, and (e) the total energies and (f) the MSDs of NbSI$_2$ with $U = 3$ eV during the AIMD simulations.

Figure S11 (a) Young's modulus and (b) Poisson's ratio of ZrSCl$_2$, (c) Young's modulus and (d) Poisson's ratio of ZrSBr$_2$, and (e) Young's modulus and (f) Poisson's ratio of ZrSI$_2$.

Figure S12 (a) Young's modulus and (b) Poisson's ratio of $ZrSCl_2$, (c) Young's modulus and (d) Poisson's ratio of $ZrSBr_2$, and (e) Young's modulus and (f) Poisson's ratio of $ZrSI_2$ under a tension of 5% along the *b*-axes.
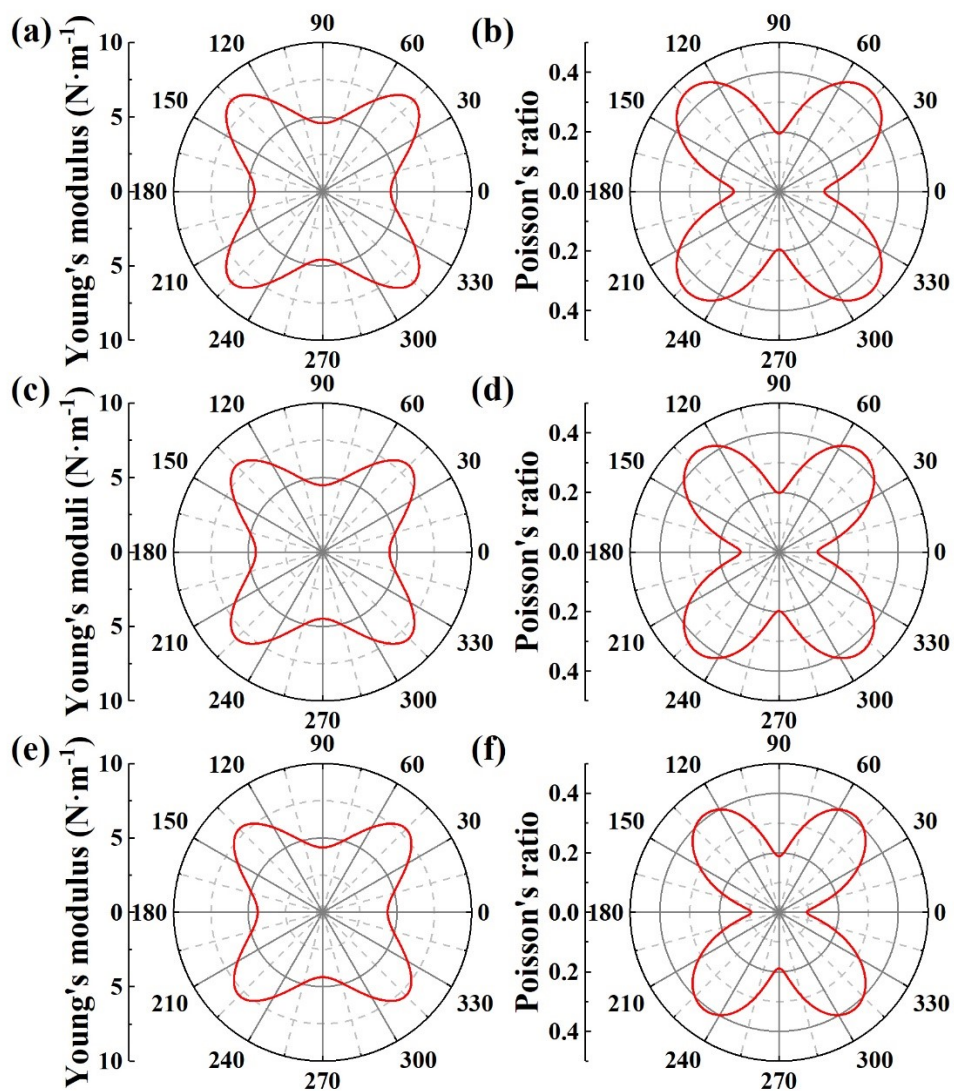
Figure S13 (a) Young's modulus and (b) Poisson's ratio of ZrSCl$_2$, (c) Young's modulus and (d) Poisson's ratio of ZrSBr$_2$, and (e) Young's modulus and (f) Poisson's ratio of ZrSI$_2$ with U = 3 eV.
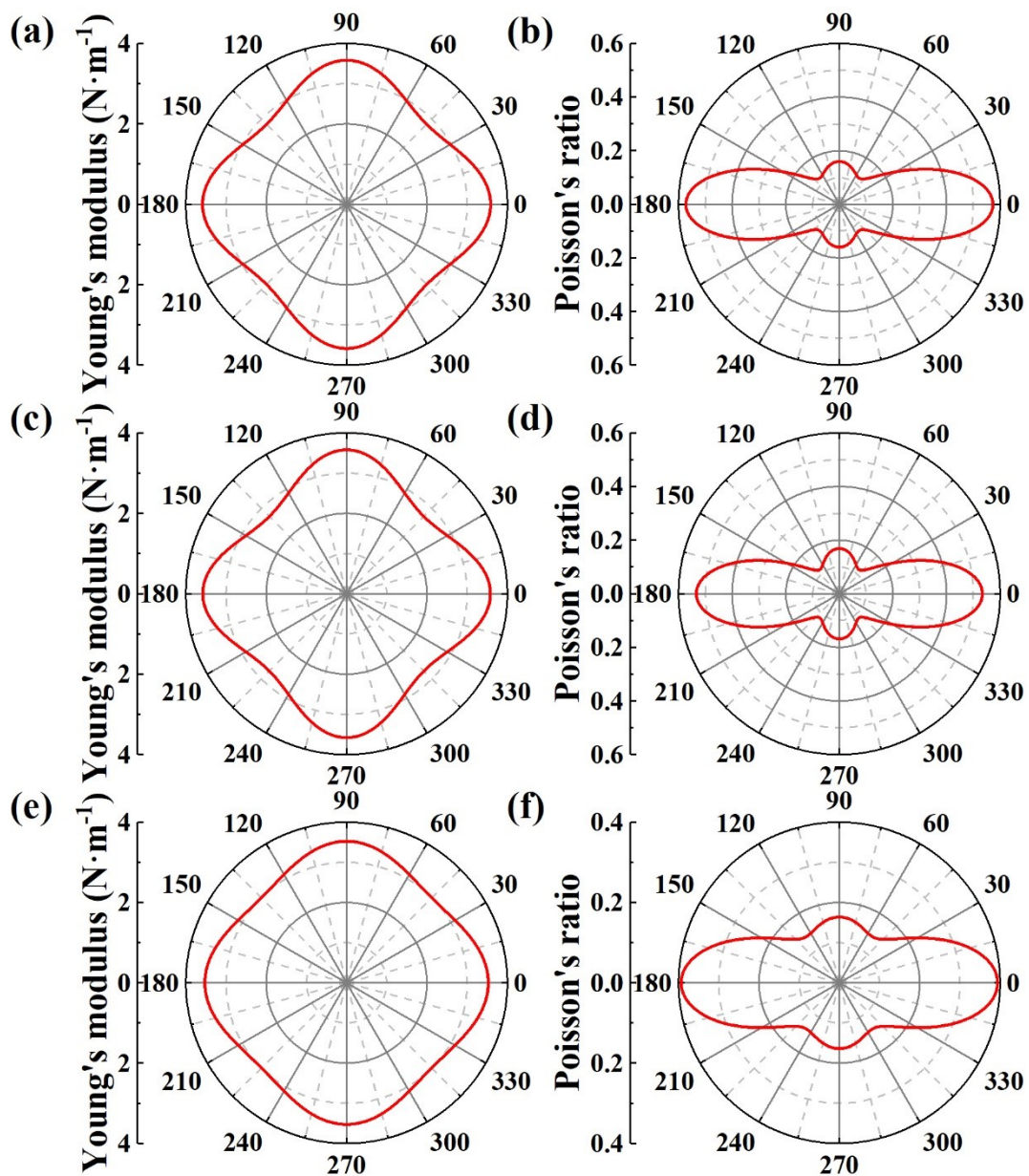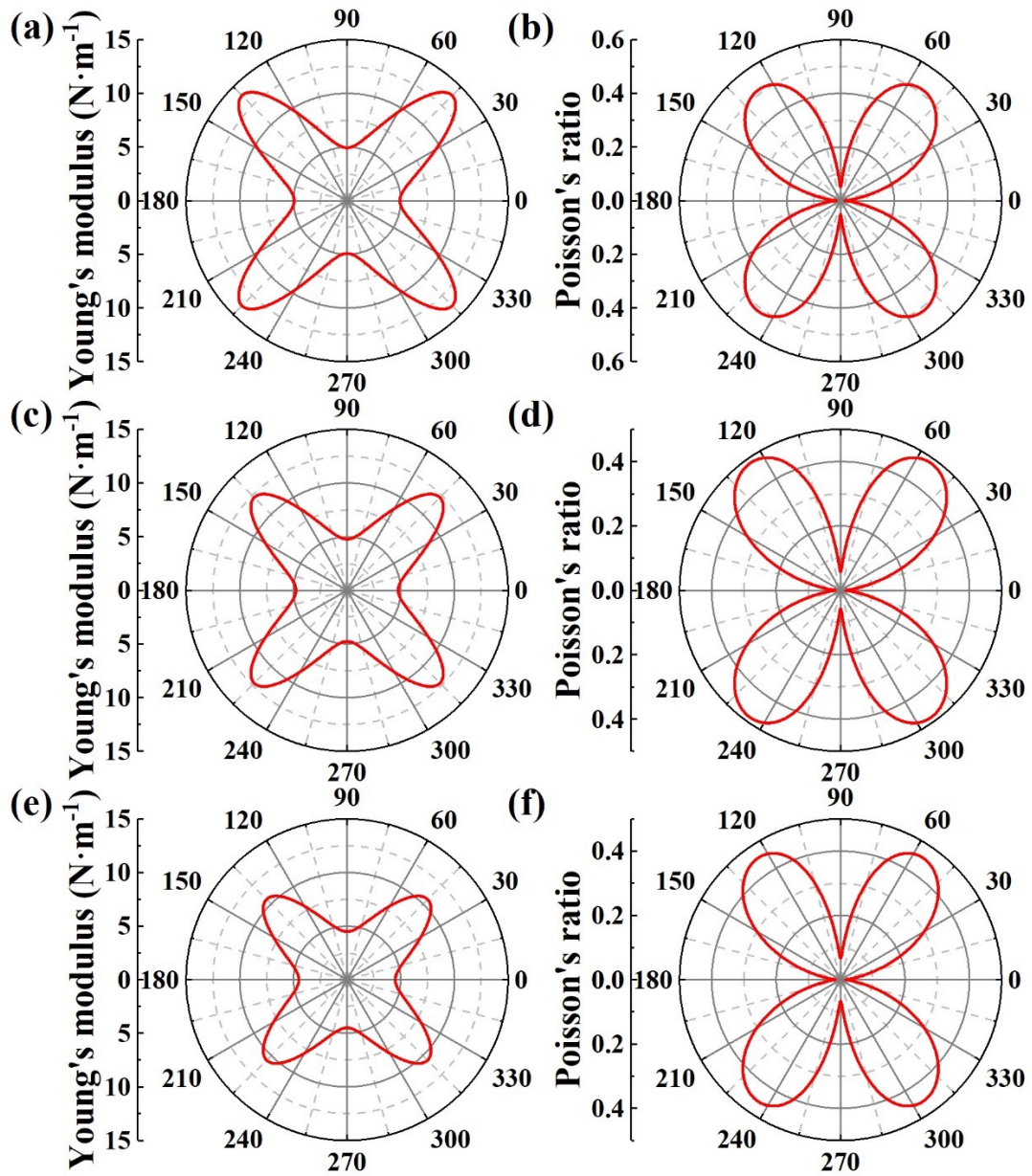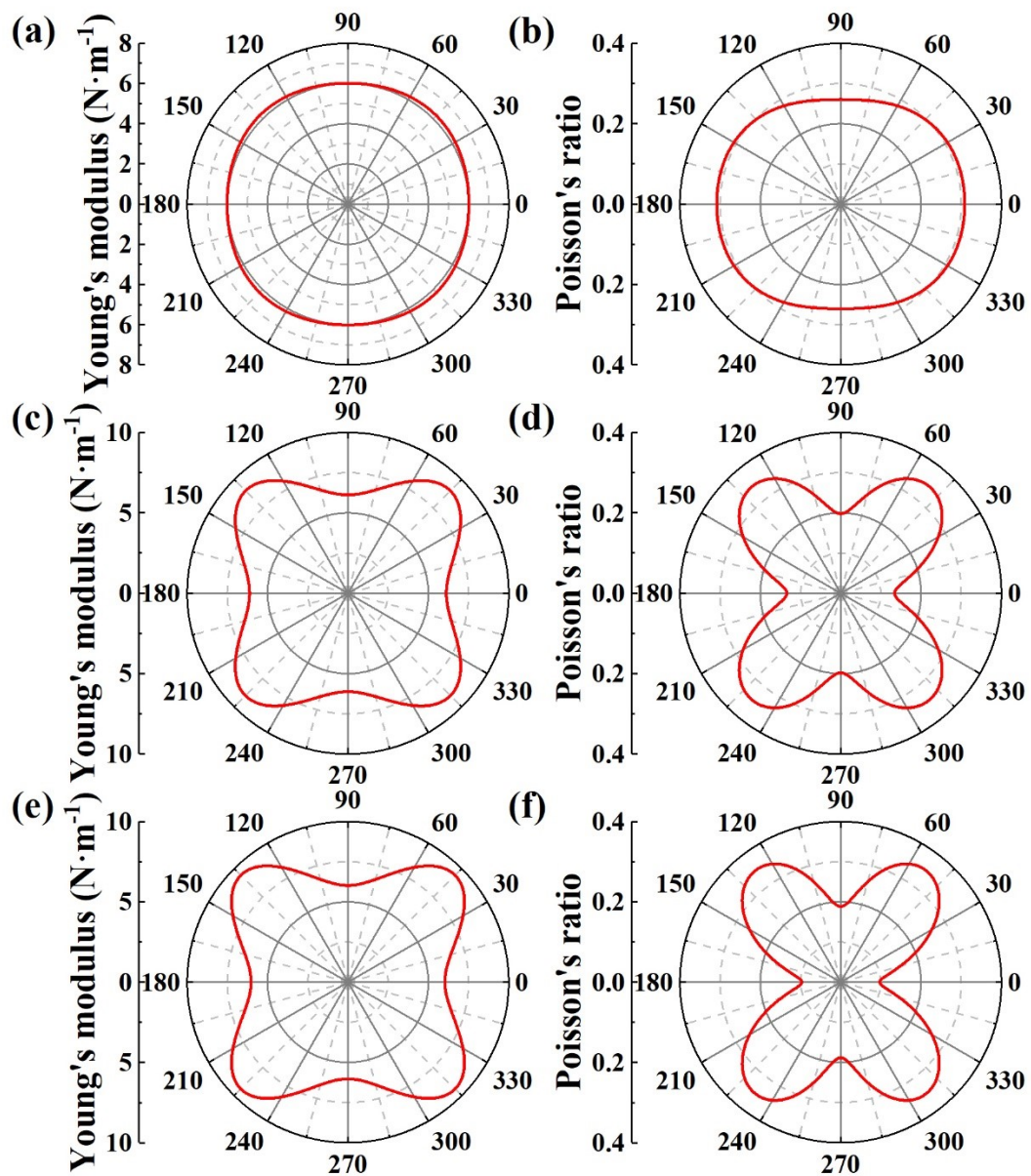
Figure S14 (a) Young's modulus and (b) Poisson's ratio of NbSCl$_2$, (c) Young's modulus and (d) Poisson's ratio of NbSBr$_2$, and (e) Young's modulus and (f) Poisson's ratio of NbSI$_2$ with U = 3 eV.
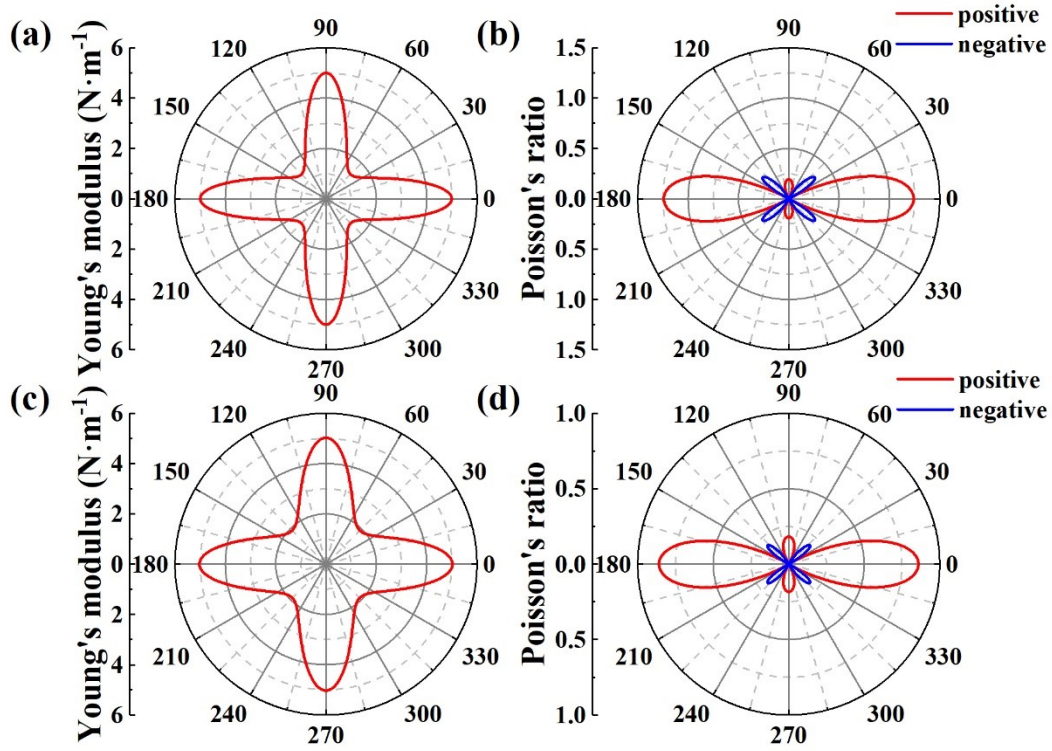
Figure S15 (a) Young's modulus and (b) Poisson's ratio of $NbSBr_2$, and (c) Young's modulus and (d) Poisson's ratio of $NbSI_2$ with $U = 3$ eV and a tension of 5% along the b-axis.

Figure S16 The energies relative to FE states as a function of step number within NEB for FE and AFE states during the ferroelastic switching in (a) $ZrSX_2$ and (b) $NbSX_2$. The inset is the energy barriers of ferroelastic switching in $NbSBr_2$ and $NbSI_2$ under a tension of 5 % along the b-axes.

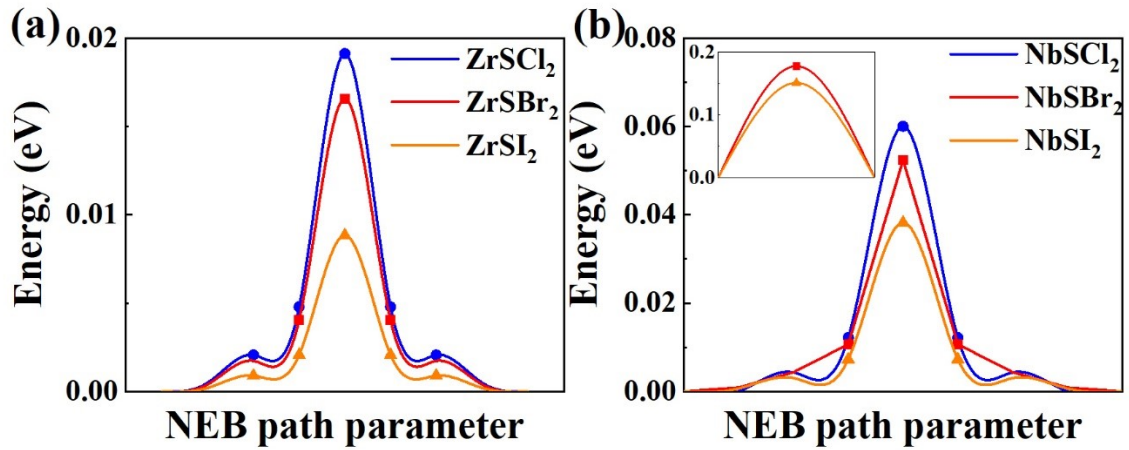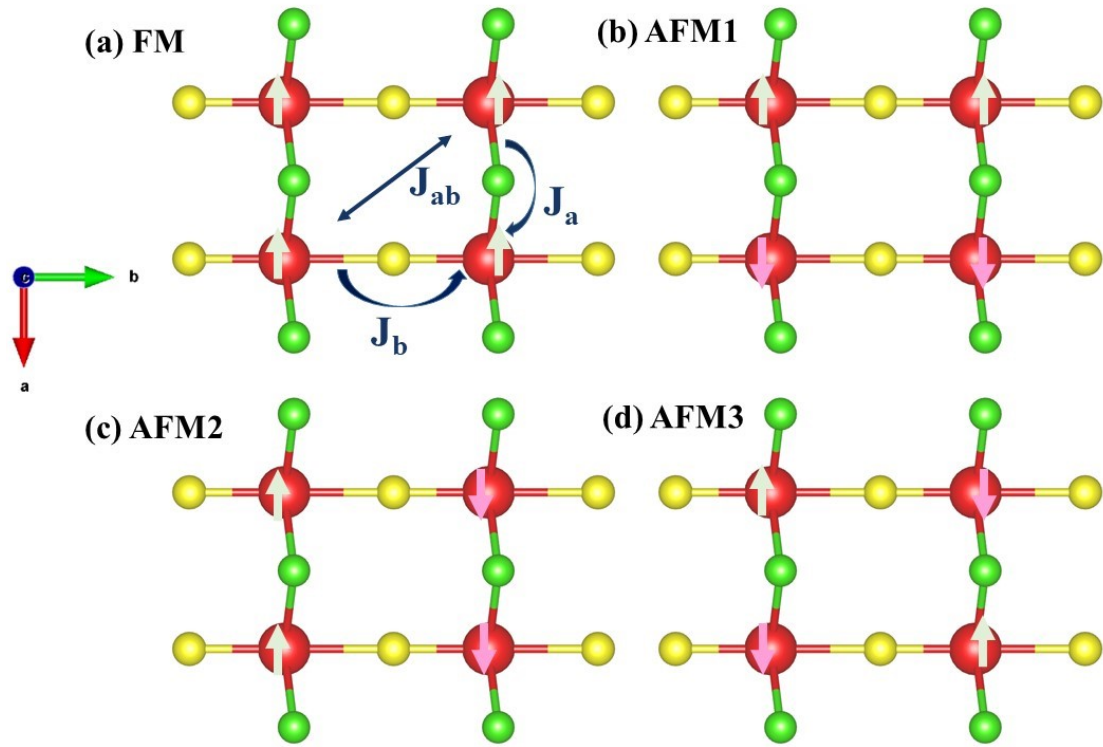Figure S17 Top views of AFM states in a 2×2×1 supercell. Red, yellow, and green spheres denote M, S, and X atoms, respectively. White and pink arrows represent the spin-up and spin-down moments, respectively.

Figure S18 MAEs of (a) NbSCl$_2$, (b) NbSBr$_2$ and (c) NbSI$_2$.
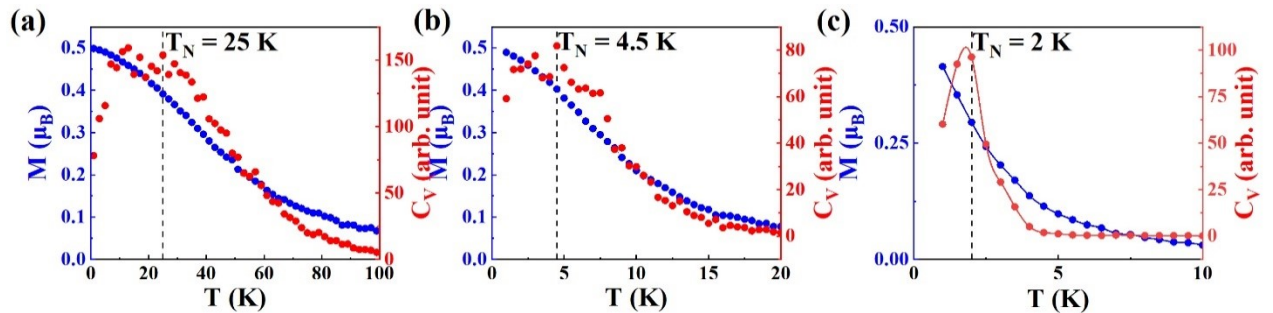
Figure S19 The simulated average magnetic moment (M) and specific heat (C$_V$) as the functions of temperature: (a) NbSCl$_2$, (b) NbSBr$_2$, and (c) NbSI$_2$.
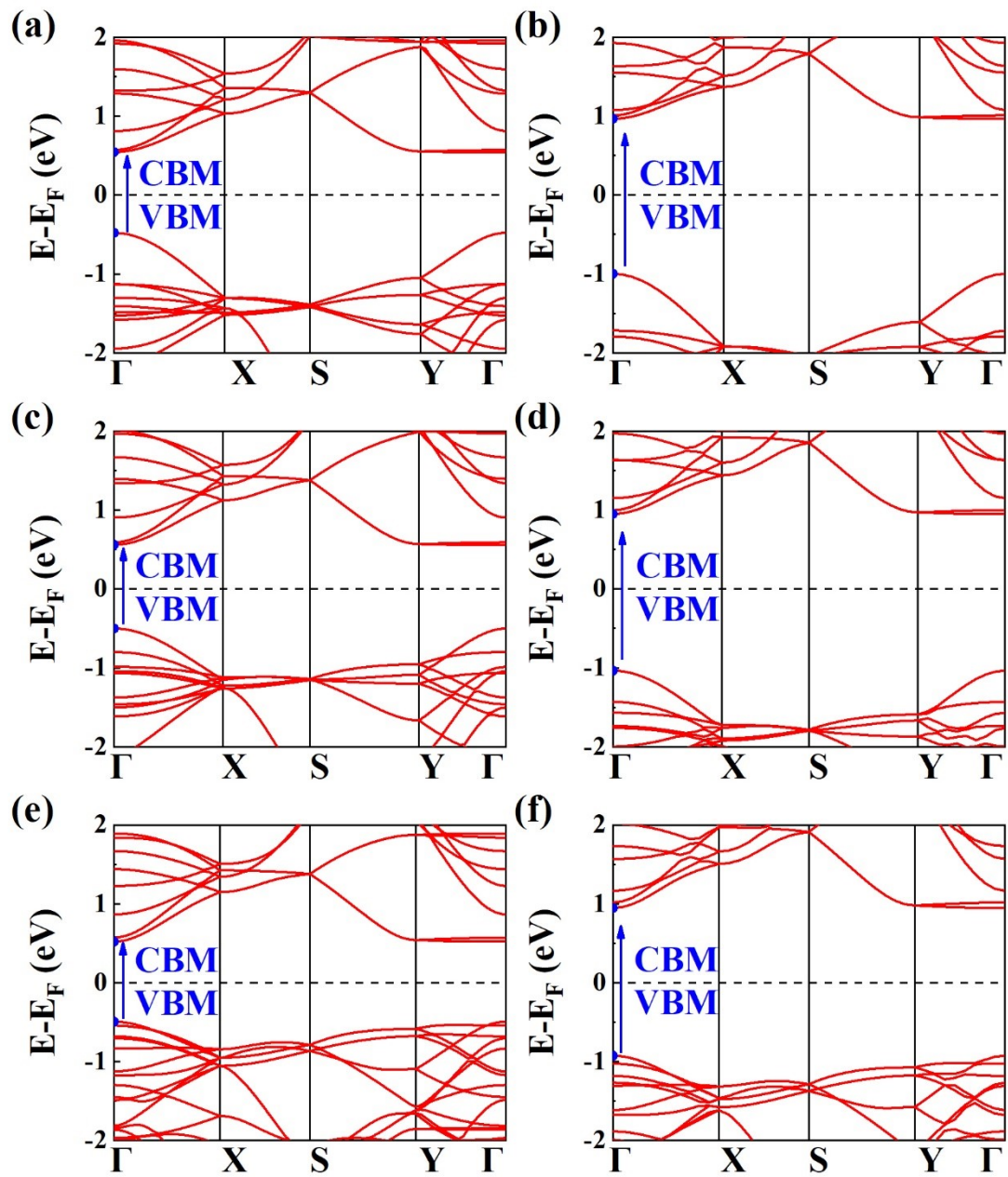
Figure S20 Band structures: FE ZrSCl$_2$ by (a) DFT and (b) HSE06, FE ZrSBr$_2$ by (c) DFT and (d) HSE06, and FE ZrSI$_2$ by (e) DFT and (f) HSE06.

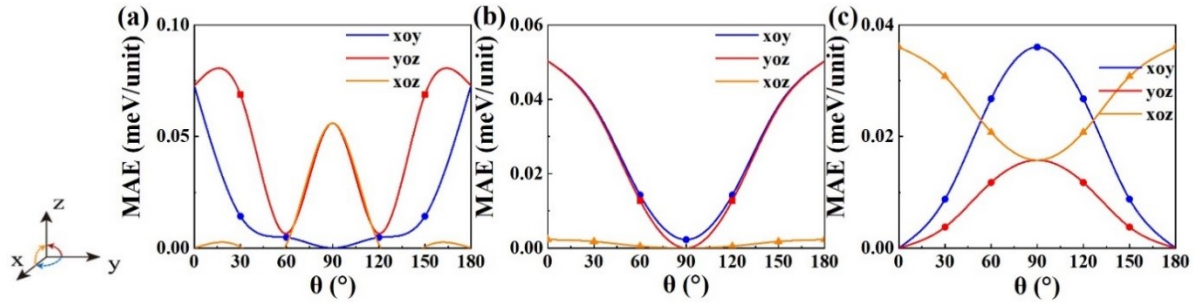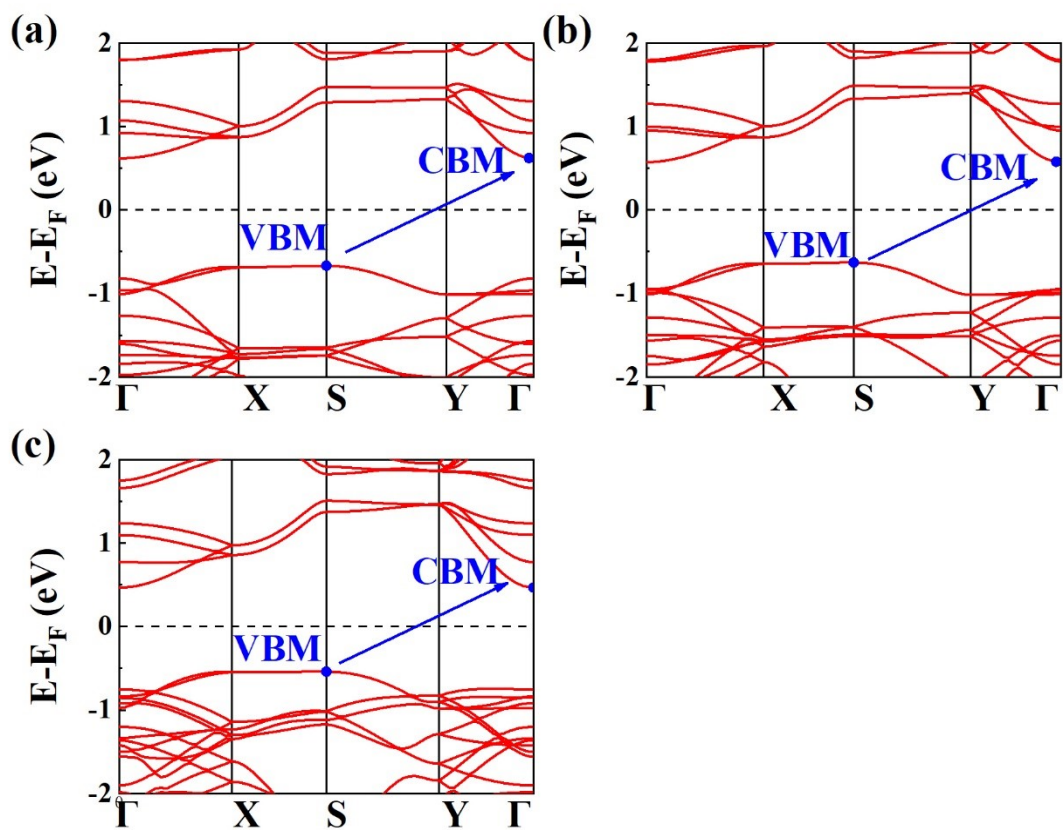Figure S21 Band structures of (a) FE NbSCl$_2$, (b) FE NbSBr$_2$, and (c) FE NbSI$_2$ by DFT+U (U = 3 eV).
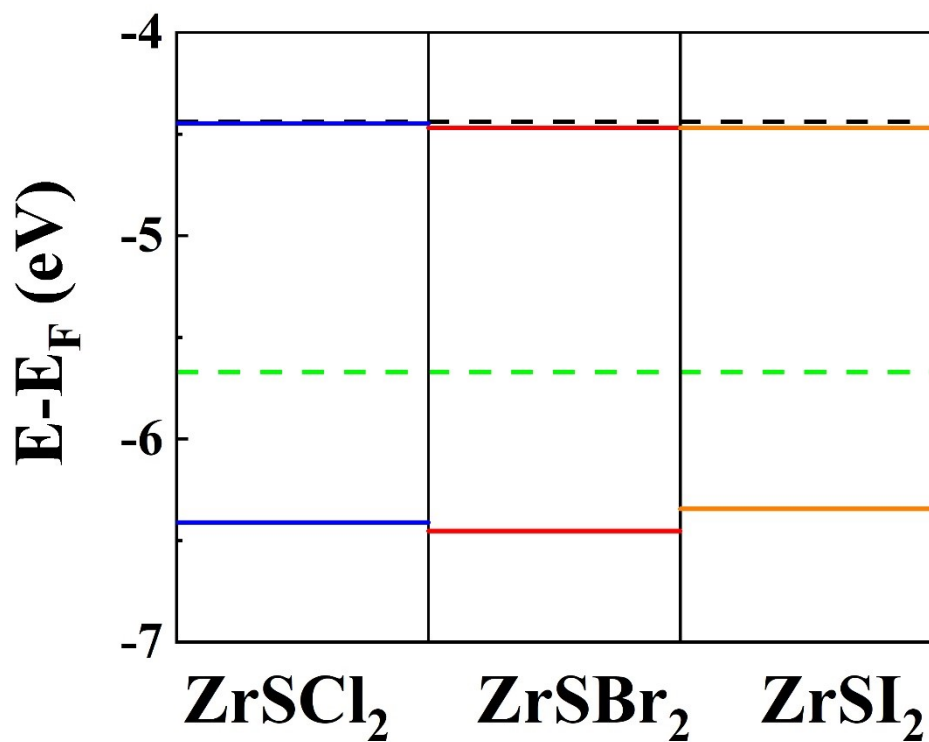
Figure S22 Band edge positions with HSE06 relative to the water redox potentials (pH = 0). positions of the reduction (H$^+$/H$_2$) and oxidation (O$_2$/H$_2$O) potentials of water are denoted by black and green dash lines, respectively.
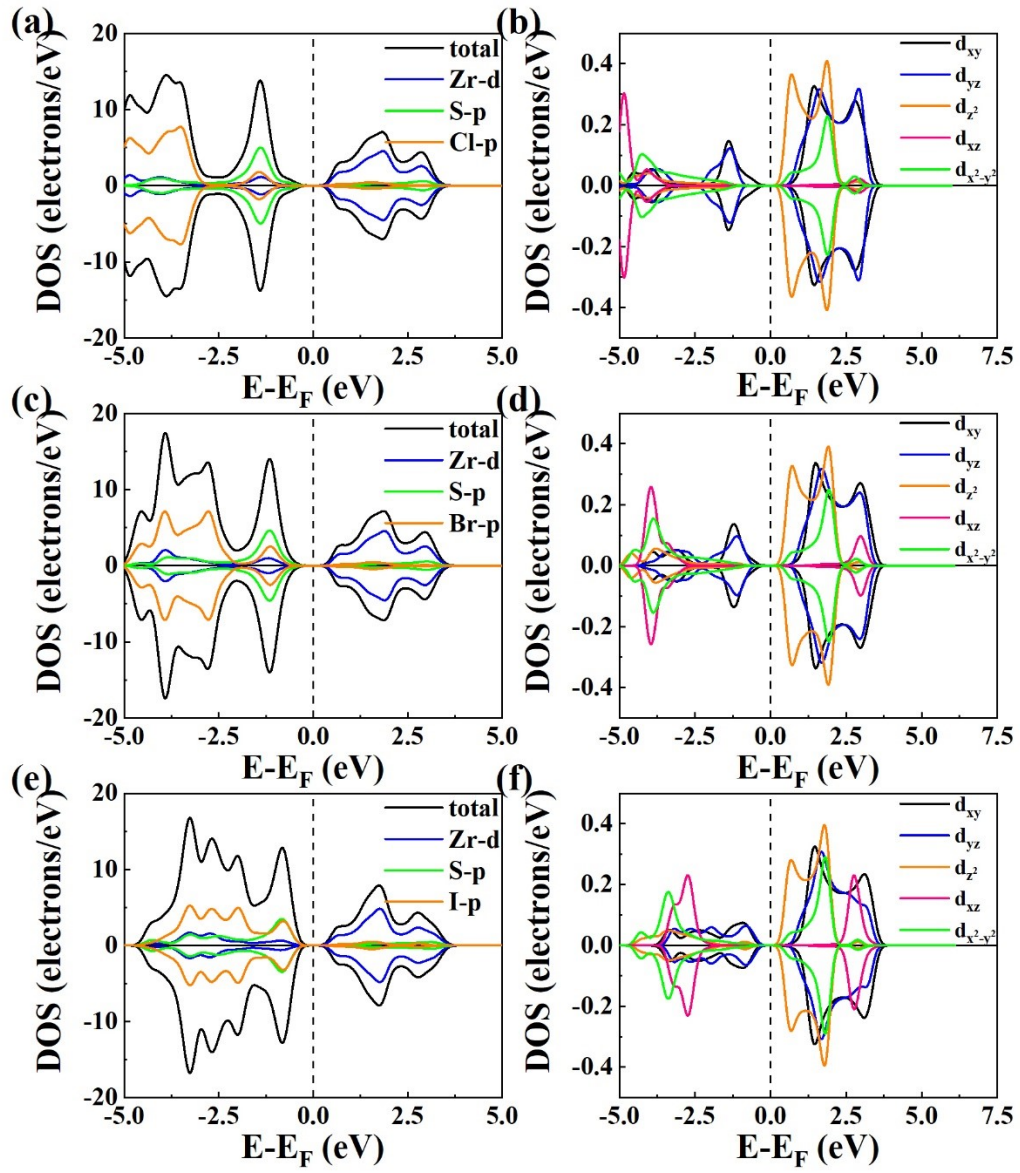
Figure S23 (a) PDOSs of ions and (b) PDOSs of the *d* electrons of Zr atoms for FE ZrSCl$_2$, (c) PDOSs of ions and (d) PDOSs of the *d* electrons of Zr atoms for FE ZrSBr$_2$, and (e) PDOSs of ions and (f) PDOSs of the *d* electrons of Zr atoms for FE ZrSI$_2$.
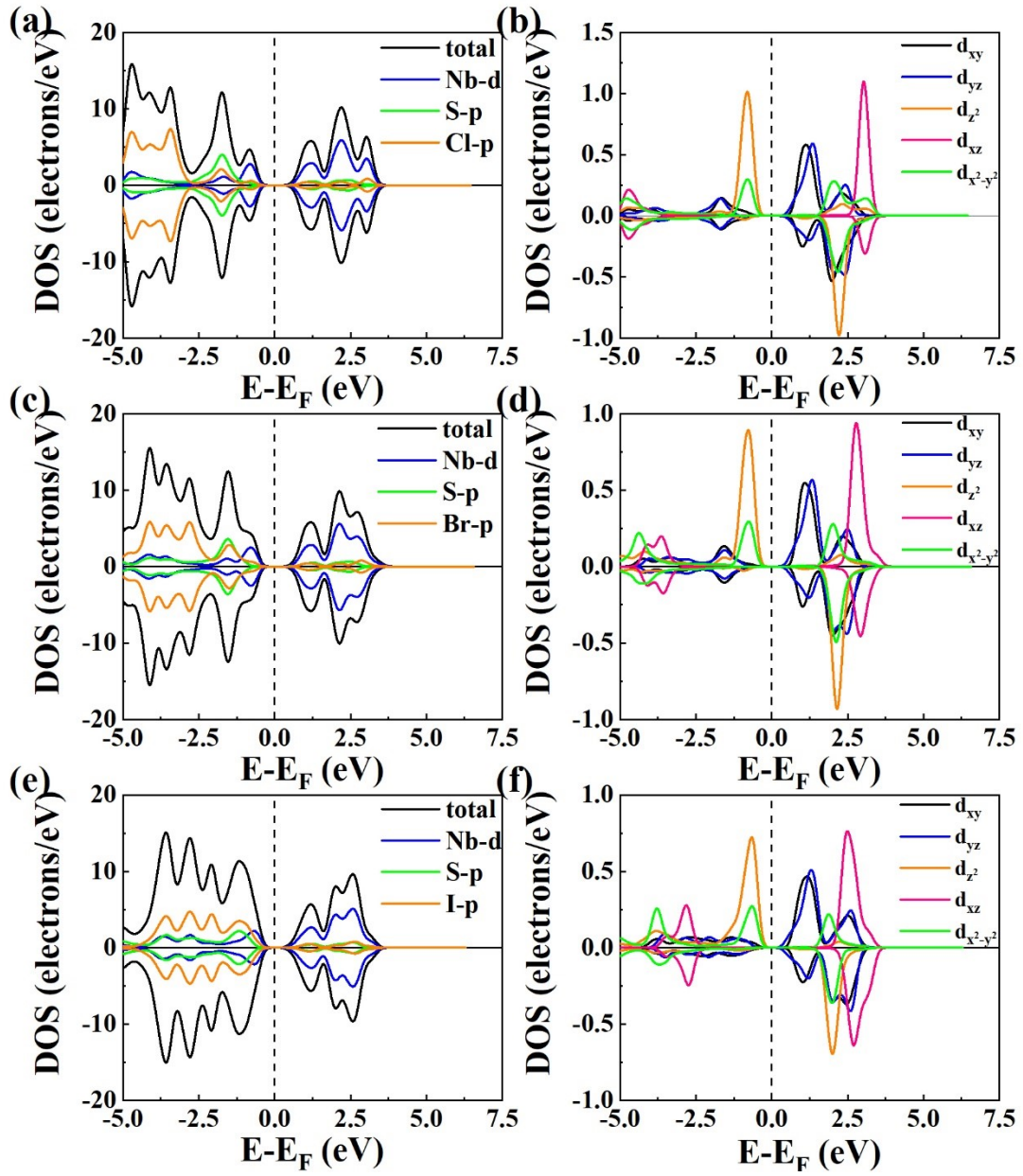
Figure S24 At U = 3 eV, (a) PDOSs of ions and (b) PDOSs of the d electrons of Nb atoms for FE NbSCl$_2$, (c) PDOSs of ions and (d) PDOSs of the d electrons of Nb atoms for FE NbSBr$_2$, and (e) PDOSs of ions and (f) PDOSs of the d electrons of Nb atoms for FE NbSI$_2$.
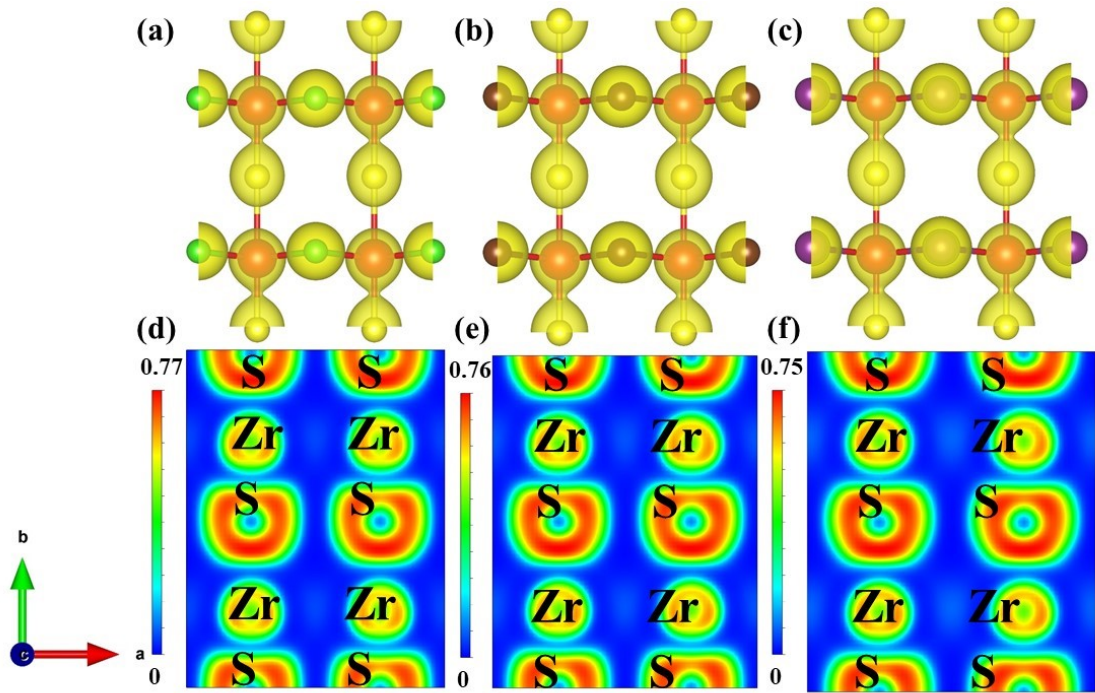
Figure S25 Top views of charge densities in FE (a) $ZrSCl_2$, (b) $ZrSBr_2$, and (c) $ZrSI_2$ and ELFs of (d) $ZrSCl_2$, (e) $ZrSBr_2$, and (f) $ZrSI_2$.
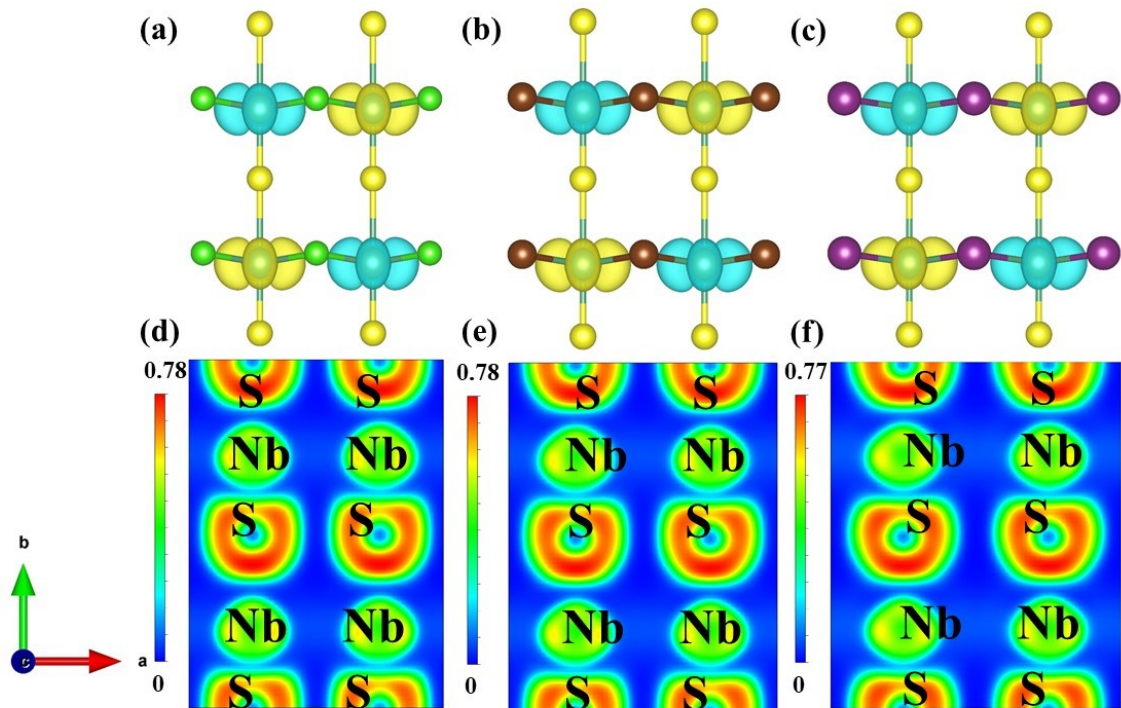
Figure S26 Top views of spin densities in FE (a) $NbSCl_2$, (b) $NbSBr_2$, and (c) $NbSI_2$ and ELFs of (d) $NbSCl_2$, (e) $NbSBr_2$, and (f) $NbSI_2$ with $U = 3$ eV. The spin-up density is shown in yellow and the spin-down density is shown in blue, respectively.
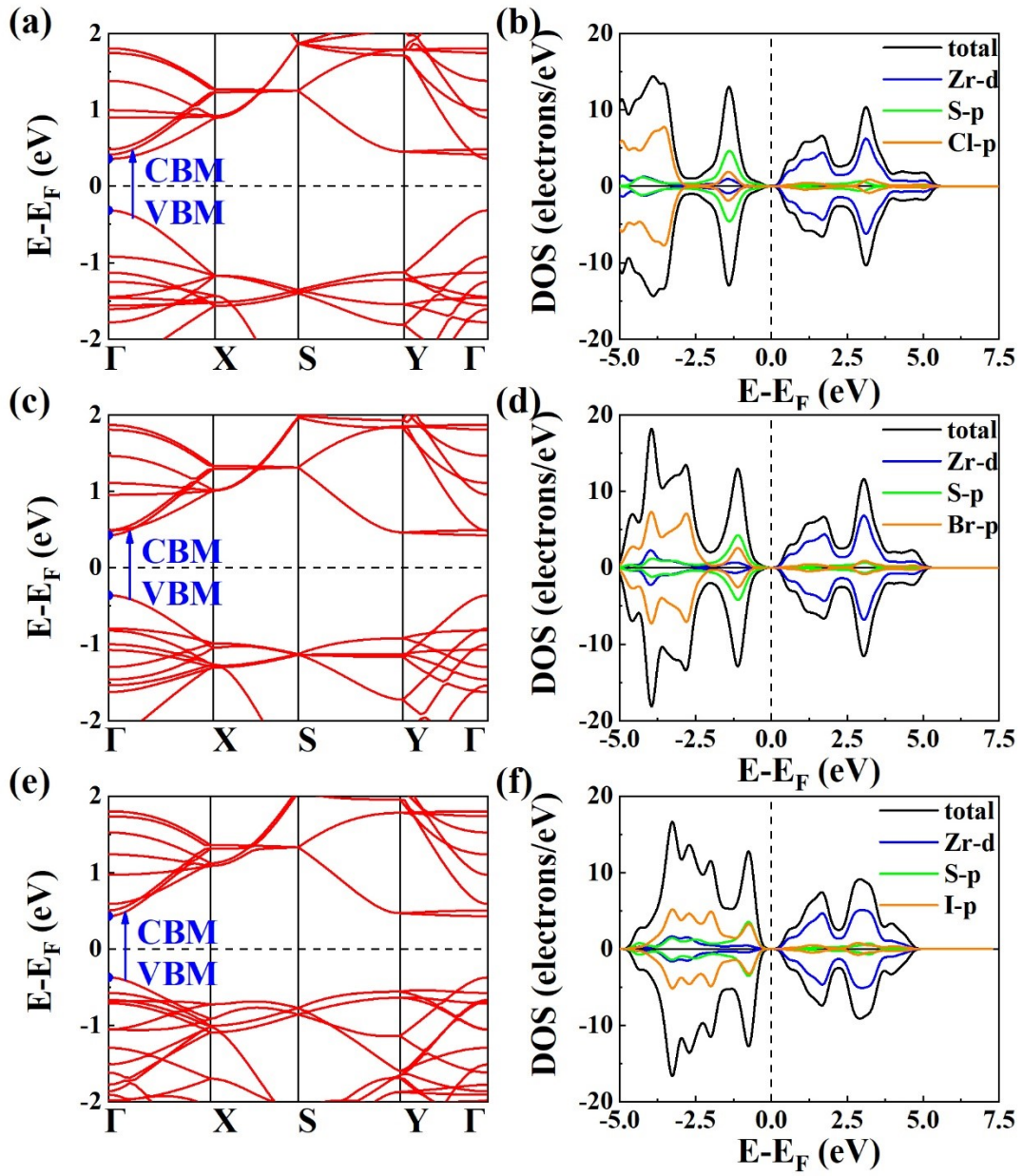
Figure S27 (a) Bands and (b) PDOSs of PE ZrSCl$_2$, (c) bands and (d) PDOSs of PE ZrSBr$_2$, and (e) bands and (f) PDOSs of PE ZrSI$_2$ without U.
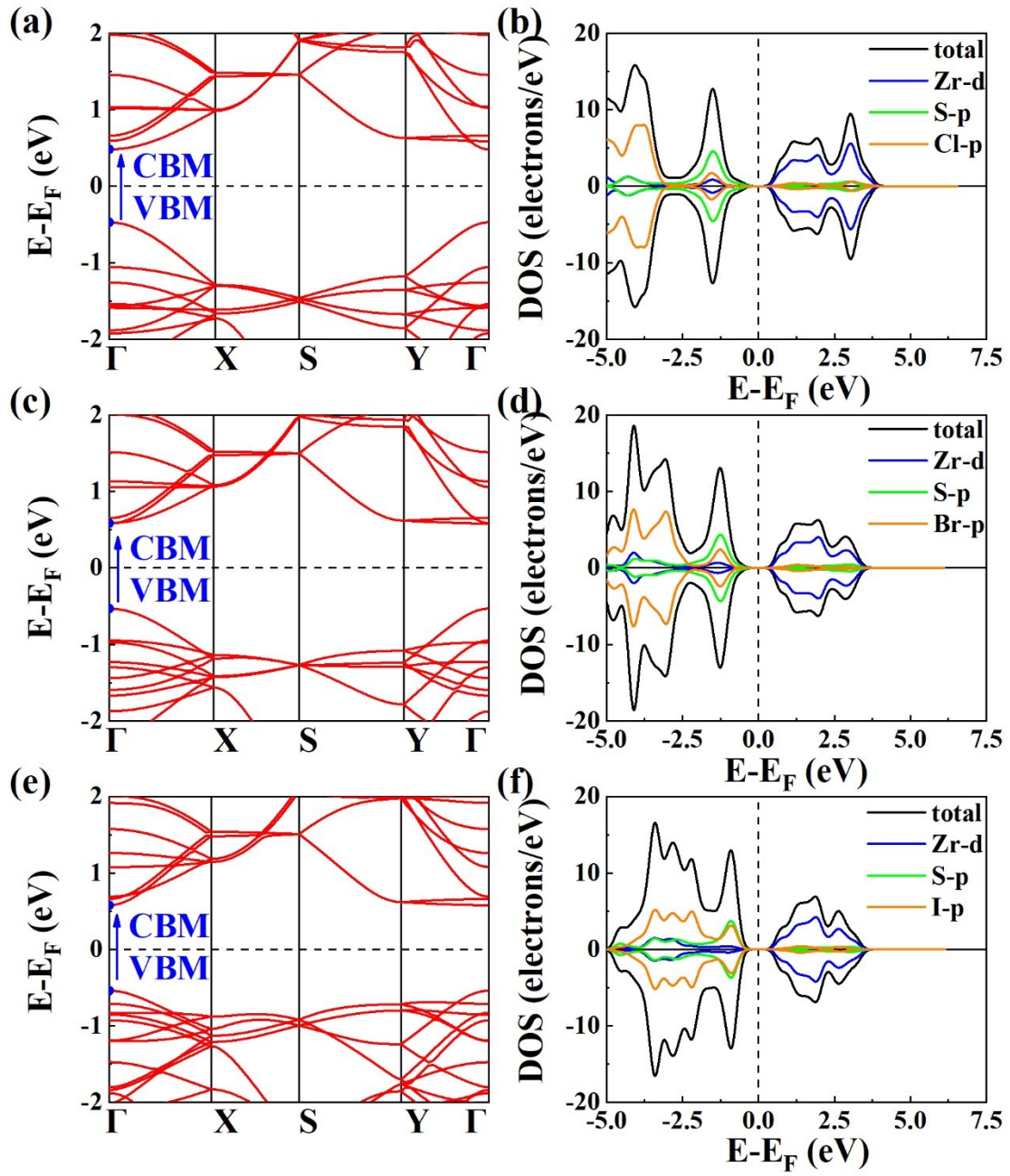
Figure S28 (a) Bands and (b) PDOSs of ZrSCl$_2$, (c) bands and (d) PDOSs of ZrSBr$_2$, and (e) bands and (f) PDOSs of ZrSI$_2$ with $U = 3$ eV.

Figure S29 (a) Bands and (b) PDOSs of PE NbSCl$_2$, (c) bands and (d) PDOSs of PE NbSBr$_2$, and (e) bands and (f) PDOSs of PE NbSI$_2$ with U = 3 eV.

Figure S30 Projected bands of Nb atoms of (a) FE and (b) PE NbSBr$_2$ with U = 3 eV.

Table S1 Lattice parameters, bond lengths, and bond angles of the proposed structures.

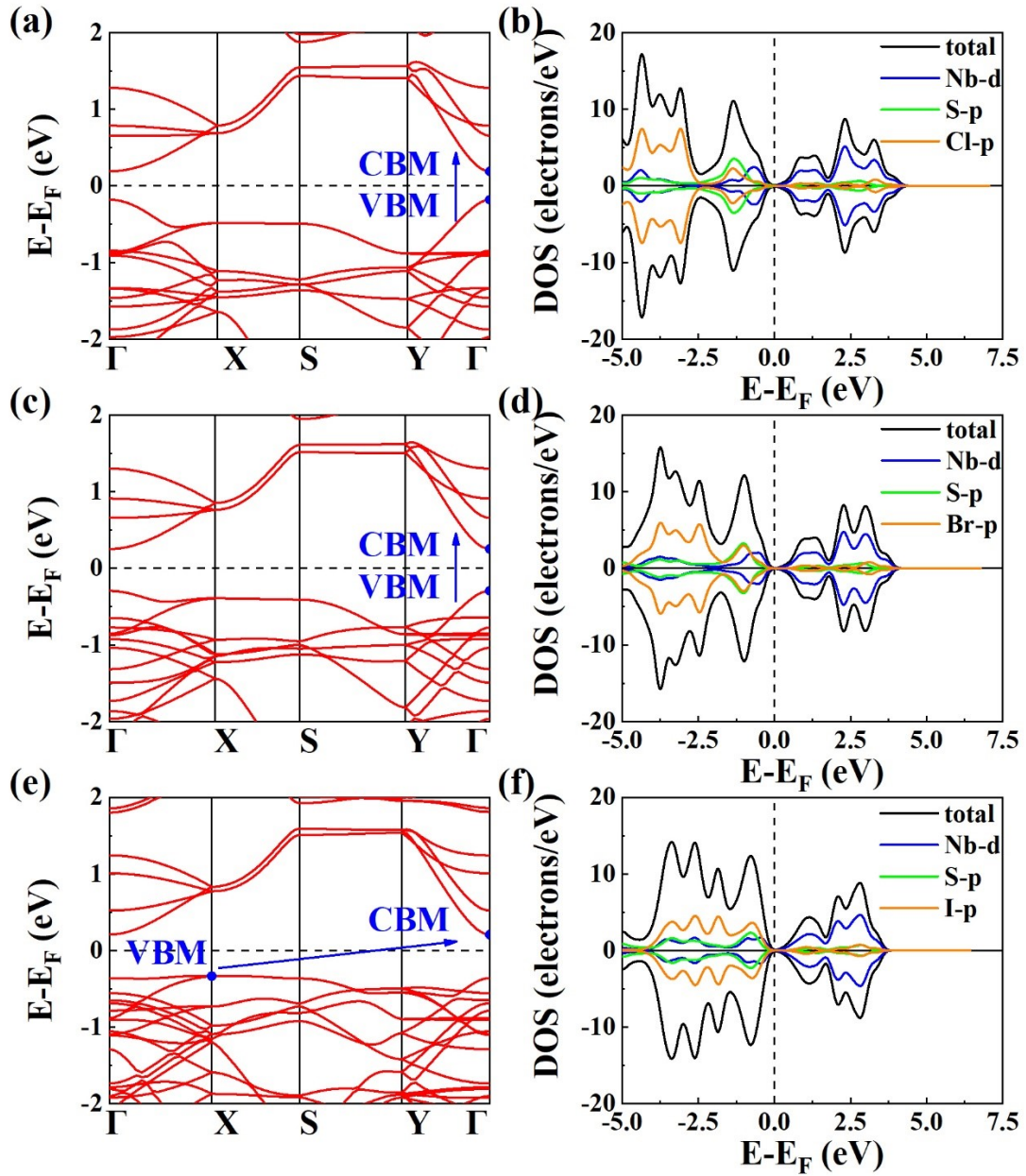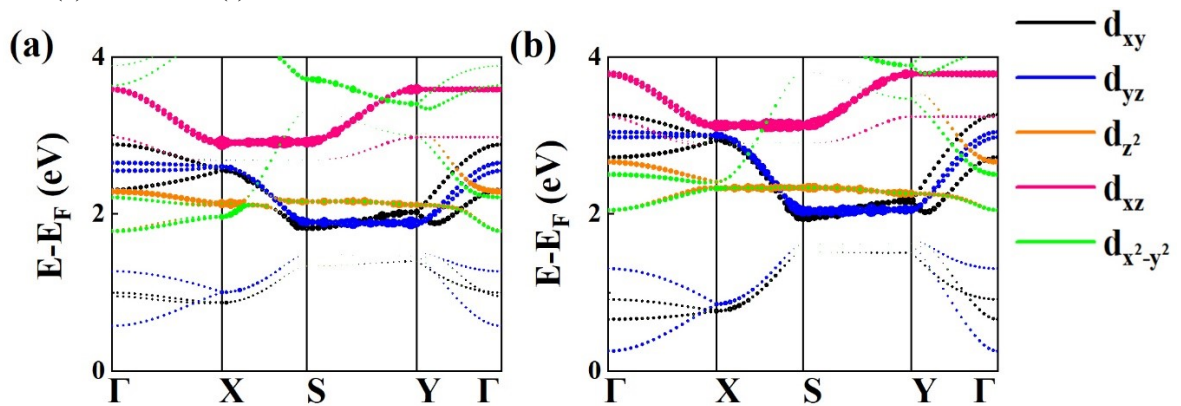| MSX$_2$	U (eV)	phase	a (Å)	b (Å)	M-S (Å)	M-S (Å)	M-X (Å)	θ$_1$ (°)	θ$_2$ (°)
ZrSCl$_2$	0	FE	3.793	4.952	2.301	2.651	2.577	95.240	84.760
ZrSCl$_2$	0	PE	3.814	4.875	2.438	2.438	2.579	90	90
ZrSCl$_2$	3	PE	3.852	4.909	2.455	2.455	2.600	90	90
ZrSBr$_2$	0	FE	3.935	4.939	2.304	2.635	2.735	95.159	84.841
ZrSBr$_2$	0	PE	3.955	4.870	2.435	2.435	2.737	90	90
ZrSBr$_2$	3	PE	3.993	4.906	2.453	2.453	2.759	90	90
ZrSI$_2$	0	FE	4.167	4.912	2.320	2.592	2.956	94.389	85.611
ZrSI$_2$	0	PE	4.181	4.864	2.432	2.432	2.958	90	90
ZrSI$_2$	3	PE	4.221	4.902	2.451	2.451	2.981	90	90
NbSCl$_2$	0	FE	3.336	4.919	2.187	2.733	2.491	97.615	82.385
NbSCl$_2$	3	FE	3.599	4.913	2.226	2.687	2.526	97.171	82.829
NbSCl$_2$	3	PE	3.643	4.775	2.388	2.388	2.532	90	90
NbSBr$_2$	0	FE	3.515	4.877	2.208	2.669	2.654	97.027	82.973
NbSBr$_2$	3	FE	3.766	4.886	2.23	2.655	2.683	96.822	83.178
NbSBr$_2$	3	PE	3.801	4.766	2.383	2.383	2.689	90	90
NbSI$_2$	0	FE	3.799	4.766	2.226	2.540	2.852	95.574	84.426
NbSI$_2$	3	FE	4.048	4.842	2.241	2.601	2.895	96.053	82.947
NbSI$_2$	3	PE	4.076	4.753	2.376	2.376	2.902	90	90

Table S2 Polar displacements of structures (Å) with different U.

MSX$_2$	$U = 0$	$U = 1$ eV	$U = 2$ eV	$U = 3$ eV
ZrSCl$_2$	0.175	0.132	0.071	0
ZrSBr$_2$	0.165	0.122	0.057	0
ZrSI$_2$	0.136	0.089	0.004	0
NbSCl$_2$	0.273	0.239	0.215	0.157
NbSBr$_2$	0.231	0.345	0.334	0.319
NbSI$_2$	0.157	0.203	0.193	0.172

Table S3 Formation energies of structures.

MSX$_2$	Tension (%)	U (eV)	E_f (eV/unitcell)
ZrSCl$_2$	0	0	-1.835
ZrSCl$_2$	5	0	-1.822
ZrSCl$_2$	0	3	-1.410
ZrSBr$_2$	0	0	-1.530
ZrSBr$_2$	5	0	-1.516
ZrSBr$_2$	0	3	-1.101
ZrSI$_2$	0	0	-1.208
ZrSI$_2$	5	0	-1.192
ZrSI$_2$	0	3	-0.775
NbSCl$_2$	0	3	-0.745
NbSCl$_2$	5	3	-0.684
NbSBr$_2$	0	3	-0.457
NbSBr$_2$	5	3	-0.437
NbSI$_2$	0	3	-0.165
NbSI$_2$	5	3	-0.147

Table S4 Formation energies of other potential phases.

MSX$_2$	U (eV)	E_{f1} (eV)	E_{f2} (eV)
ZrSCl$_2$	0	-1.970	-0.431
ZrSCl$_2$	3	-2.330	-0.731
ZrSBr$_2$	0	-0.869	-0.451
ZrSBr$_2$	3	-1.217	-0.710
ZrSI$_2$	0	0.320	-0.534
ZrSI$_2$	3	-0.012	-0.792
NbSCl$_2$	3	-1.664	-0.768
NbSBr$_2$	3	-0.635	-0.923
NbSI$_2$	3	0.435	-1.091

Table S5 Energies (eV) and lattice parameters (Å) of ZrSX$_2$ with and without spin.

ZrSX$_2$	Including spin	U (eV)	Energy (eV)	a (Å)	b (Å)
ZrSCl$_2$	yes	0	-22.472	3.793	4.952
ZrSCl$_2$	no	0	-22.472	3.793	4.952
ZrSBr$_2$	yes	0	-21.128	3.935	4.939
ZrSBr$_2$	no	0	-21.128	3.935	4.939
ZrSI$_2$	yes	0	-19.741	4.167	4.912
ZrSI$_2$	no	0	-19.741	4.167	4.912

Table S6 Energies (eV) of AFM states of $NbSX_2$.

$NbSX_2$	FM	AFM1	AFM2	AFM3
$NbSCl_2$	-78.310	-79.211	-78.285	**-79.214**
$NbSBr_2$	-73.979	-74.119	-73.968	**-74.123**
$NbSI_2$	-68.980	-69.043	-68.961	**-69.049**

Table S7 Bandgaps of the proposed structures.

MSX_2	phase	method	Band gap (eV)
$ZrSCl_2$	FE	DFT	1.022
$ZrSCl_2$	PE	DFT	0.674
$ZrSCl_2$	PE	DFT+U, U = 3 eV	0.954
$ZrSCl_2$	FE	HSE06	1.963
$ZrSBr_2$	FE	DFT	1.059
$ZrSBr_2$	PE	DFT	0.787
$ZrSBr_2$	PE	DFT+U, U = 3 eV	1.112
$ZrSBr_2$	FE	HSE06	1.984
$ZrSI_2$	FE	DFT	1.015
$ZrSI_2$	PE	DFT	0.803
$ZrSI_2$	PE	DFT+U, U = 3 eV	1.118
$ZrSI_2$	FE	HSE06	1.873
$NbSCl_2$	FE	DFT+U, U = 3 eV	1.287
$NbSCl_2$	PE	DFT+U, U = 3 eV	0.369
$NbSBr_2$	FE	DFT+U, U = 3 eV	1.204
$NbSBr_2$	PE	DFT+U, U = 3 eV	0.547
$NbSI_2$	FE	DFT+U, U = 3 eV	1.006
$NbSI_2$	PE	DFT+U, U = 3 eV	0.538

Table S8 Bond angles of proposed structures with and without tension (°).

MSX_2	U (eV)	Tension (%)	θ_1	θ_2	α_1	α_2	$(\alpha_1+\alpha_2)/2$
$ZrSCl_2$	0	0	95.240	84.760	94.765	84.276	89.521
$ZrSCl_2$	0	5	98.085	81.915	94.790	82.932	88.861
$ZrSBr_2$	0	0	95.159	84.841	92.007	87.067	89.537
$ZrSBr_2$	0	5	98.133	81.867	92.113	85.590	88.852
$ZrSI_2$	0	0	94.389	85.611	89.629	89.701	89.665
$ZrSI_2$	0	5	97.719	82.281	89.805	88.127	88.966
$NbSBr_2$	3	0	96.822	83.178	89.156	89.227	89.192
$NbSBr_2$	3	5	98.909	81.091	93.421	83.820	88.621
$NbSI_2$	3	0	96.053	82.947	88.726	90.000	89.363
$NbSI_2$	3	5	98.308	81.692	92.200	85.403	88.802